Available online at www.sciencedirect.com
ScienceDirect
Journal of Power Sources 163 (2007) 695–701
JOURNAL OF POWER SOURCES
www.elsevier.com/locate/jpowsour

Electrocatalysis of methanol, ethanol and formic acid using a Ru/Pt metallic bilayer

Sherlan G. Lemos [a], Robson T.S. Oliveira [a], Mauro C. Santos [a], Pedro A.P. Nascente [b], Luís O.S. Bulhões [a,c], Ernesto C. Pereira [a,*]

[a] *Departamento de Química, Universidade Federal de São Carlos, C.P.: 676, CEP 13565-905, São Carlos, SP, Brazil*
[b] *Departamento de Engenharia de Materiais, Universidade Federal de São Carlos, São Carlos, SP, Brazil*
[c] *CENIP, Centro Universitário Central Paulista, UNICEP, São Carlos, SP, Brazil*

Received 22 July 2006; received in revised form 29 September 2006; accepted 29 September 2006
Available online 17 November 2006

Abstract

This work describes the methanol, ethanol and formic acid oxidation using a metallic bilayer electrodeposited on a platinum substrate. Firstly, one monolayer of ruthenium was deposited on the substrate and over it a 1.1 layer of metallic platinum. In the blank solution it was observed that the electrochemical behavior of both the Pt/Ru/Pt and bulk Pt were very similar, except in the oxygen evolution potential region. Using X-ray photoelectronic spectroscopy (XPS) it was not possible to identify the presence of Ru atoms on the bilayer surface. The electroactive area and the RMS roughness factor measured with atomic force microscopy (AFM) for both materials are the same. A CO monolayer oxidation procedure confirmed that the systems have the same real surface area and also showed a shift in the negative direction for 54 mV on the CO peak potential for the bilayer. For the voltammetric organic molecules oxidation, an enhancement in the current densities of 350, 390 and 420% was observed for ethanol, methanol and formic acid, respectively, for the bilayer system compared to the bulk Pt electrodes. Also, a decrease of 110 mV in the beginning of the ethanol oxidation process was observed over the bilayer system compared to bulk Pt.

Keywords: Ruthenium; Platinum; Small organic molecules; Oxidation; Nanotechnology

1. Introduction

Nowadays, the search for new sources of energy is important due to finite availability of fossil fuel reserves and also due to environmental concerns. In this context, fuel cells are a valuable option since they have high energy efficiency and low pollutant emission [1–5]. Different kinds of small organic molecules, such as methanol, and ethanol can be used as fuel. The main problem concerning the use of small organic molecules as fuel is that CO is an intermediate in the oxidation pathway [6–10]. This species adsorbs strongly on the platinum surface. Therefore, different authors have investigated the reaction mechanism and also the development of new electrode materials aiming at the identification of the intermediate species, the reaction byproducts and the displacement of the processes towards more negative potentials [11]. In this sense, most of the papers in the literature describe the methanol oxidation [12–19]. During the oxidation process, the electrocatalyst must break the C–H bond enabling the reaction of the intermediate products (CO, H_2CO and HCOOH) with an O containing species leading to CO_2 at low potentials [7]. In the case of ethanol oxidation the catalyst must also break the C–C bond [20–22].

A simple and successful alternative to decrease the CO poisoning effect is the addition of supporting elements to Pt, ruthenium being employed most frequently. Other elements such as Sn and Rh have also been studied [23,24]. These elements provide the generation of O containing species at low potentials compared to pure Pt. This phenomenon is the well-known bifunctional mechanism, where the intermediate adsorbed products (CO_{ads}, as an example) react with hydroxilated species [25].

Recently, a new approach to the development of electrocatalysts has been proposed by our group [26,27]. We prepared multilayers of noble metals which have enhanced properties compared to pure metals or alloys [26,27]. The magnetic and

* Corresponding author. Tel.: +55 16 3351 8214; fax: +55 16 3351 8214.
E-mail address: decp@power.ufscar.br (E.C. Pereira).

0378-7753/$ – see front matter © 2006 Elsevier B.V. All rights reserved.
doi:10.1016/j.jpowsour.2006.09.058

electronic properties of multilayers have been widely studied in the literature and new attributes have been observed which are generically described as spintronic behavior [28]. From a theoretical point of view, Norskov and co-workers have investigated several aspects of the properties of metals and alloys [29–34]. These authors show that the CO adsorption energy is related to the substrate d-energy level. Recently, a paper was published that describes the effect of a platinum monolayer over different single crystals materials for the oxygen reduction reaction [35]. There, the electrocatalytical effect observed was also discussed based on d-orbitals level energy.

Our results for the bilayers show an improvement for the current density voltammetric peaks for small organic molecules oxidation up to 380% compared to flat polycrystalline Pt [26,27]. The same behavior was observed for the chronoamperometric measurements. These results indicate a decrease of the surface poisoning related to strongly bonded adsorbates. In the present paper, we prepared a new bilayer system based on a Ru/Pt deposited over a polycrystalline Pt substrate. The Pt layer was the metal exposed to the solution. We chose ruthenium due to the important literature results using this element alloyed to Pt as an electrocatalyst for small organic molecules oxidation. The bilayer system was characterized using X-ray photoelectronic spectroscopy (XPS), atomic force microscopy (AFM) and electrochemical techniques.

2. Experimental

Initially, the Pt electrodes were mechanically polished down to 1 μm with diamond paste and rinsed with acetone and a large amount of purified water (Milli-Q® system). Subsequently, one Ru monolayer was electrodeposited on the polycrystalline Pt substrate (geometric area = 0.2 cm^2) at 0.05 V versus hydrogen electrode in the same solution (HESS) during 300 s using a 1.0×10^{-3} mol L^{-1} $RuCl_3 \cdot 3H_2O$ solution in 0.1 mol L^{-1} H_2SO_4. After Ru deposition the electrode was rinsed prior to Pt deposition and placed in the Pt solution on an open circuit potential (ocp). Even at ocp it was not observed Ru dissolution prior Pt deposition. A 1.1 Pt monolayer was obtained over the Ru layer using a 5.0×10^{-4} mol L^{-1} H_2PtCl_6 in 0.1 mol L^{-1} $HClO_4$ solution. This electrodeposition was carried out at 0.05 V for 20 s. The thickness of the metal layers was calculated by the integration of the charge passed during the electrodeposition. Two Pt sheets with 2 cm^2 each were used as auxiliary electrodes. The small organic molecules oxidation was investigated in a 0.1 mol L^{-1} perchloric and 0.1 mol L^{-1} sulphuric media, using cyclic voltammetry and chronoamperometry. All the current densities are referred to electroactive area, which was calculated using the well-known procedure (hydrogen UPD desorption charges), obtaining a value of 0.38 cm^2. Also, CO oxidation was performed to compare the catalytic properties of the two systems and verify their real surface areas. CO was adsorbed onto the polycrystalline Pt electrode by bubbling CO gas in a 0.1 mol L^{-1} perchloric acid solution for 30 min. Solution CO was subsequently removed by bubbling high purity nitrogen gas for 30 min holding the potential at 0.05 V. The potential was then cycled starting at 0.05 V for one complete oxidation/reduction cycle. To check the reproducibility, the electrodes preparation and electrochemical experiments were performed twice at room temperature. The chronoamperometric oxidation data were measured at 0.5 V for ethanol and formic acid, and 0.6 V for methanol. The organic concentrations in the solutions were 0.5 mol L^{-1} for ethanol and methanol, and 1.0 mol L^{-1} for formic acid. All the solutions were prepared using analytical grade reagents and Milli-Q® system purified water.

An EG&G PARC 263 potentiostat was used in the electrochemical measurements. The monolayers were characterized by X-ray photoelectron spectroscopy and atomic force microscopy. XPS measurements were performed on freshly prepared Pt/Ru/Pt surfaces in ultra-high vacuum (low 10^{-7} Pa range) using a Kratos XSAM HS spectrometer. Non-monochromatic Al Kα ($h\nu$ = 1486.6 eV) radiation was used as X-ray source, emission current of 12 mA at a voltage of 14 kV. High-resolution spectra were obtained with analyser energy of 20 eV. Shirley background, mixed Gaussian/Lorentzian functions and a least-square routine were used for the fitting to the peaks. AFM images and the roughness measurements were performed using a scanning tunneling microscope Digital Instruments (DI) Multimode AFM/STM controlled by Nanoscope III system (DI).

3. Results and discussion

3.1. Preparation and characterization of the Ru/Pt bilayer over Pt substrate

Fig. 1 shows the AFM micrographs for both Pt substrate (Fig. 1a) and Ru/Pt bilayer (Fig. 1b). To calculate the roughness mean square, five regions were measured on the surfaces

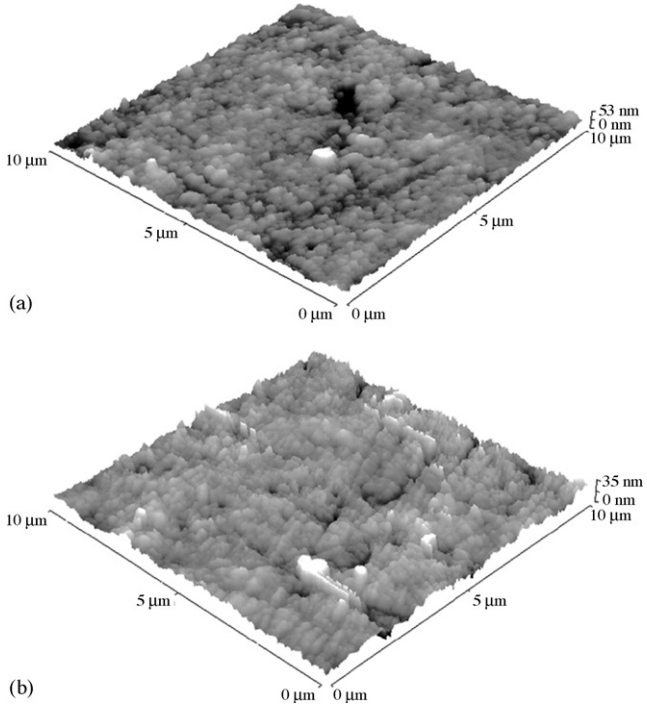

Fig. 1. AFM images for: (a) Pt substrate and (b) Ru/Pt bilayer eletrodeposited over Pt.

Table 1
Roughness mean square (RMS) values for Pt substrate and for Ru/Pt bilayer obtained from AFM images

Sample	RMS (Pt)	RMS (Pt/Ru/Pt)
1	4.9452	5.1243
2	7.1236	6.6323
3	6.4561	7.6546
4	8.3321	7.2351
5[a]	7.9553	8.2421
Mean	6.9624 ± 1.3428	6.9736 ± 1.1913

[a] Value measured in the center of the sample.

and no differences were observed comparing the bilayer and the substrate within the experimental error considering a *t*-test at a 95% confidence level (Table 1). Therefore, any differences in the electrochemical behavior cannot be correlated to the surface area changes.

Fig. 2a displays XPS Pt 4f spectrum, associated to Pt^0 with a minor contribution of Pt oxides. A spin-orbit-split doublet of Ru $3d_{5/2}$ and Ru $3d_{3/2}$ at 280.3 and 284.5 eV, respectively, which are characteristic of metallic ruthenium [36], were not observed in Fig. 2b indicating that Ru was not detected. However, the XPS penetrates up to six monolayers deep into the sample depending on the incidence angle. This lack of sensitivity likely results

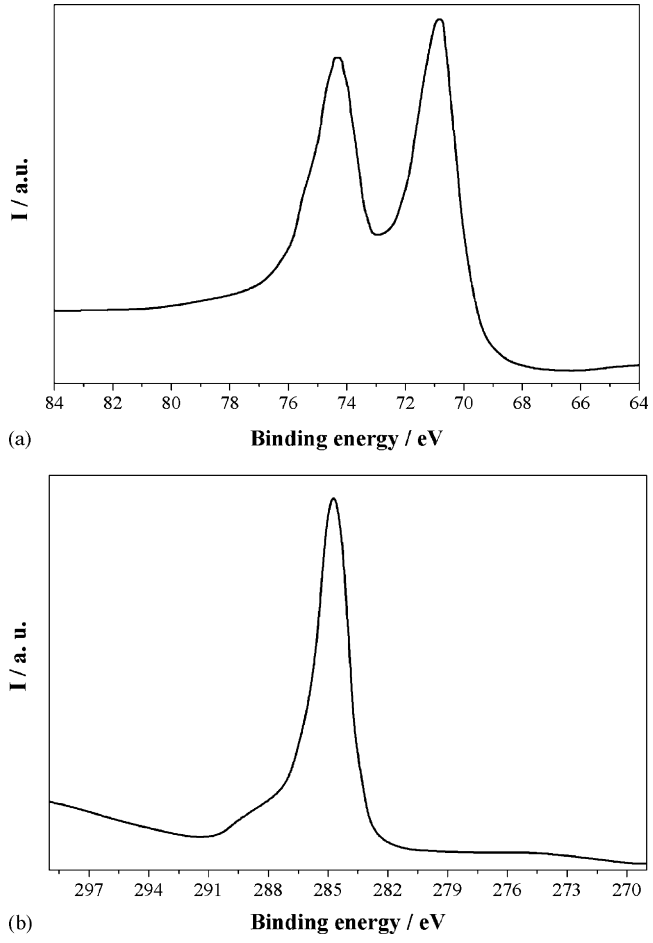

Fig. 2. XPS spectra for Ru/Pt bilayer electrodeposited over Pt: (a) XPS Pt 4f spectrum and (b) XPS C 1s spectrum.

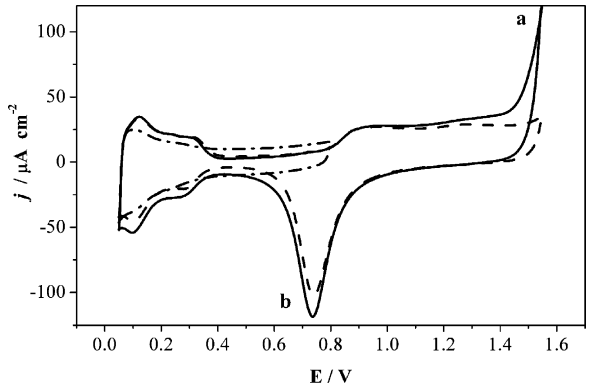

Fig. 3. Cyclic voltammograms for Pt electrode (dashed line), Ru/Pt bilayer over Pt (solid line) and Ru monolayer (dot–dashed line) in 0.1 mol L^{-1} $HClO_4$, scan rate = 100 mV s^{-1}.

from the small amount of Ru present in the underlayer and the presence of carbon impurities. The prominent peak in Fig. 2b, at around 285, is related to C 1s due to organic contaminants from sample preparation or cleaning, which hinders the ruthenium detection. Otherwise, the electrochemical data allows, as discussed below, show that probably there is not Ru atoms on the active surface.

The voltammetric characterization of the Pt/Ru/Pt bilayer, Ru monolayer and Pt electrodes in $HClO_4$ are presented in Fig. 3. In order to obtain a reproducible surface, prior to the experiments, the electrodes (except for Ru monolayer electrode) were cycled between 0.05 and 1.55 V at 1.0 V s^{-1} for 300 cycles. The electroactive areas were equal for all substrates. The observed voltammetric behavior of the bilayer was very similar to the polycrystalline Pt up to 1.2 V. For more positive potentials, the oxygen evolution reaction over the bilayer is observed (Fig. 3, region a). This phenomenon is associated with an electrocatalytical effect characteristic of the bilayer since no ruthenium reduction was observed during the negative potential sweep (Fig. 3, region b). Additionally, the Ru monolayer voltammetric profile is characteristic of a bulk ruthenium electrode [37] and quite different to that one presented for the bilayer. It is interesting to point out that the effect on the water oxidation was not observed for the case of Rh/Pt bilayer [26,27]. The electroactive surface area calculated corroborated those results obtained with AFM micrographs, i.e., there is no change in the surface area. Thus, despite the two elements present very similar physical–chemical characteristics (since, they are side by side in the periodic table), their associations with platinum as a metallic bilayer present very different electrochemical characteristics.

It should be pointed out here that the results described above and in the whole work were obtained for a metallic bilayer prepared starting from a $RuCl_3$ solution aged for 3 days. When the bilayer was formed, starting from a recently prepared solution, it had different electrocatalytical properties comparing to a bilayer prepared starting from an aged ruthenium solution. Besides, this was identified by the disappearance of the oxygen evolution reaction. Thus, we used the oxygen evolution reaction to characterize the success of the bilayer formation. We are not proposing that the bilayer has not been formed starting from a

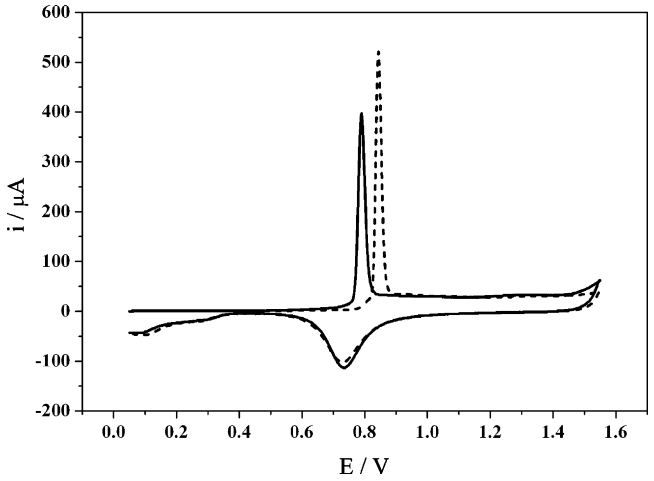

Fig. 4. Cyclic voltammograms obtained for the oxidative stripping of a CO monolayer on polycrystalline Pt (dashed line) and on the bilayer Ru/Pt electrodeposited over Pt (solid line) in 0.1 mol L^{-1} $HClO_4$. Sweep rate: 100 mV s^{-1}.

recently prepared solution, but, that those bilayers possess different properties.

One possible explanation is that using a $RuCl_3$ recently prepared solution, the ruthenium adsorption over Pt occurs starting from the complex $Ru(H_2O)_6^{3+}$ and it is driven through the specific adsorption of chloride [38]. When that solution is aged for 3 days, ruthenium species suffer hydrolysis generating ruthenil species – $[RuO(H_2O)_4]^{2+}$ – in acid media [39,40]. The kinetics of the adsorption on the polycrystalline platinum is similar, but not the mechanism [41].

In order to stress the bilayer characterization, a CO monolayer oxidative stripping procedure was performed to establish the real surface areas of these two catalysts. Also, this procedure gives support to a possible verification of the Ru presence on the outer Pt layer, once CO_{ads} stripping voltammetry is quite sensitive to the presence of small amounts of Ru atoms that may be present on the surface. Fig. 4 summarizes our results for the stripping voltammetry of essentially saturated monolayers of CO_{ads} on Pt (dashed line) and Ru/Pt bilayer (solid line). As one can see, the profiles for both systems are very similar. CO_{ads} oxidation over Pt showed a sharp and symmetric oxidation peak centered at approximately 0.84 V, in agreement with literature data [42,56]. In contrast, others studies also on polycrystalline Pt reported the oxidation peak centered at lower potentials [43–46]. These authors [42,56] attributed their results to the predominance of one crystallographic orientation on the electrode surface. CO_{ads} oxidation over Ru/Pt bilayer showed also a symmetric sharp peak centered, however, at 0.79 V. The peak widths measured at peak half height were 0.02 V for Pt and 0.03 V for Ru/Pt bilayer. CO_{ads} oxidation in the case of Ru traces on the electrode surface leads to a characteristic broad profile and a peak potential shift of about 0.19 V towards negative potentials, being higher depending on Ru coverage and/or preparation procedure (alloy or spontaneous deposition) [43–46]. The electrochemical active surface areas, assuming a monolayer CO_{ads} stripping charge of 420 μC cm^{-2}, were 0.31 and 0.32 cm^2 for Pt and Ru/Pt bilayer system. So, one can conclude, from CO oxidation procedure, that there is no change in the electrochemical active surface area. These results are in agreement with the AFM micrographs presented in Fig. 1 and Table 1.

3.2. Evaluation of the Ru/Pt bilayer on the small organic molecules oxidation

Fig. 5 shows the voltammetric profiles for the ethanol, methanol and formic acid oxidations on the polycrystalline Pt electrode (dashed line) and on the Ru/Pt bilayer (solid line) and for methanol oxidation over the Ru monolayer. All the determinations were performed in 0.1 mol L^{-1} $HClO_4$ and 0.1 mol L^{-1} H_2SO_4 media, presenting the typical oxidation profiles [47–64].

Ethanol oxidation is presented in Fig. 5a. Two oxidation peaks, centered at 0.85 (peak 1) and 1.25 V (peak 2), are observed during the positive potentials sweep and a reactivation peak is observed during the negative sweep. The first peak appears in a region of potentials where OH bonded to the Pt surface is formed quickly, through the gradual current increase that follows the hydrogen desorption [47]. The formation of OH species plays an important role during the ethanol oxidation, explained by a dual path mechanism, with break of the C–C bond, producing CO_2 via the CO strongly adsorbed on the platinum substrate [47,48]. It is important to point out that not only strongly adsorbed species but also weakly bonded intermediates are present at the Pt surface. Also weakly adsorbed species contribute to blocking surface impeding OH formation and inhibiting those pathways that require additional oxygen atoms for oxidation [49]. The second peak during the positive sweep is caused by the CO_2 and by other products as acetic acid and acetaldehyde, the latter one being the main product in ethanol concentrations above 0.2 mol L^{-1} [49,50].

Fig. 5b shows the methanol oxidation, which presents typical profile characterized by the inhibition of the hydrogen adsorption/desorption region, and beginning oxidation at potentials above 0.40 V, with current density peaks in 0.85 (peak 1) and 1.35 V (peak 2) during the positive sweep. In the negative sweep, the current shows an increase starting at 0.85 V with a peak around 0.75 V (peak 3), then falling to zero at potentials below 0.40 V. The inhibition of the hydrogen adsorption/desorption peaks occurs due to the methanol adsorption in the same potential region (0.05–0.40 V). The first anodic process is attributed to the oxidative removal of adsorbed/dehydrogenated methanol fragments (CO_{ads}, as an example) by PtOH species [51,52]. During this process, CO, CO_2, HCOH, HCOOH and $HCOOCH_3$ are formed and the CO molecule readsorbes, poisoning the surface [7,53]. This process is followed by a decline in the current density due to the formation of surface oxide [54]. The second anodic process (peak 2) can be associated with the oxidation of the species produced over the surface oxide [53–56]. During the negative potentials sweep, methanol and other adsorbed species suffer re-oxidation at 0.75 V, on a recently revealed Pt surface after the removal of the oxide layer [54]. For methanol oxidation on Ru monolayer in both electrolytes, it is observed that the current density was too low as expected for a ruthenium electrode [37] (Fig. 5b).

Formic acid oxidation is presented in Fig. 5c. Three peaks are observed in the positive sweep at approximately 0.6, 0.9

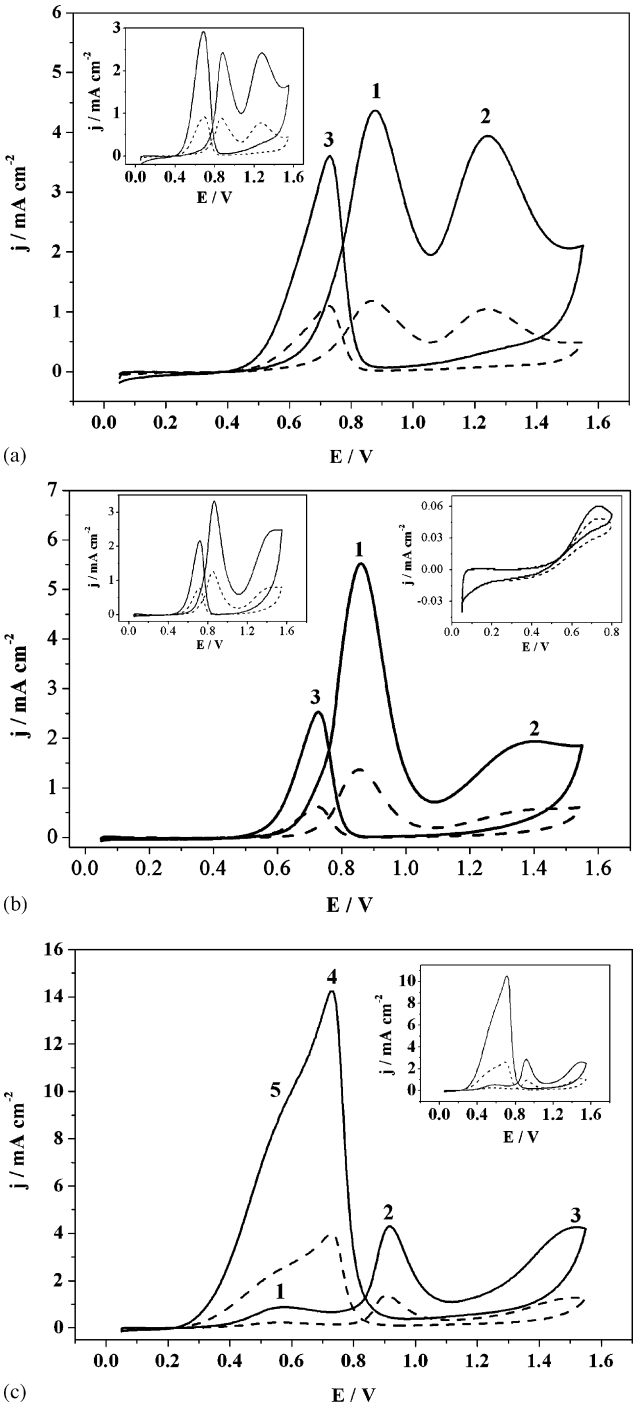

Fig. 5. Cyclic voltammograms obtained for the oxidation of: (a) 0.5 mol L^{-1} ethanol, (b) 0.5 mol L^{-1} methanol and (c) 1.0 mol L^{-1} formic acid in 0.1 mol L^{-1} $HClO_4$ (larger graph) and H_2SO_4 0.1 mol L^{-1} (insert), on polycrystalline Pt (dashed line) and on the bilayer Ru/Pt electrodeposited over Pt (solid line). Sweep rate: 20 mV s^{-1}. The right insert in Fig. 5b is related to the oxidation of 0.5 mol L^{-1} methanol over a Ru monolayer in 0.1 mol L^{-1} $HClO_4$ (solid line) and H_2SO_4 0.1 mol L^{-1} (dashed line).

and 1.5 V (peaks 1–3, respectively); two peaks during the negative sweep at 0.7 and 0.5 V (peaks 4 and 5) are also observed. HCOOH eletroxidation on platinum electrodes has CO_2 [57–59] as main product and CO_{ads} as predominant byproduct [10,60–63]. Similar to MeOH and EtOH oxidation processes,

Table 2
Current density increases (in %) for the small organic molecules oxidation over Pt/Ru/Pt system compared to Pt ($n = 2$) in the two electrolyte solutions

Organic molecule	Sulphuric acid	Perchloric acid
Ethanol	269 ± 9	347 ± 29
Methanol	253 ± 17	394 ± 14
Formic acid	346 ± 4	422 ± 38

For methanol and ethanol, the first peak of the positive potentials sweep was considered ($E_p = 0.85$ V), and the second one for formic acid ($E_p = 0.92$ V).

the hydrogen adsorption/desorption charges are suppressed, indicating that the superficial active Pt sites were blocked by the presence of organic adsorbates. The first anodic peak near to 0.6 V can be attributed to HCOOH oxidation in the surface sites that remained unblocked after CO adsorption [62]. During the second anodic peak, CO_{ads} oxidation is involved. However, the charge for adsorbed CO oxidation is smaller than the observed in that current peak, suggesting that another species oxidation occurs, probably the HCOOH direct oxidation [63]. In higher potentials, some catalytic active sites of surface oxides are formed, creating a third anodic peak near 1.5 V [64]. During the negative potentials sweep, the surface remains inactive until the partial reduction of the oxide formed. The oxidation peak 4 presents the real catalytic activity of the Pt surface, since neither CO nor oxides are present in the surface [63]. Finally, the second peak of the negative sweep (shoulder at around 0.5 V) can be attributed to an influence of CO_{ads} and contribution of its oxidation [63].

An examination of the organic molecules oxidation over the Ru/Pt bilayer (solid lines in Fig. 5) reveals no changes in the current density peak potentials in relation to polycrystalline Pt substrate. It is important to point out that these results do not necessarily imply that the reaction mechanisms are the same for the Ru/Pt bilayer and Pt. However, Fig. 5 shows an increase in the global current density, both in perchloric and sulphuric acid media. Table 2 presents the percentage increase in the current density observed for the first peak of the positive potentials sweep for methanol and ethanol ($E_p = 0.85$ V), and the second one for formic acid ($E_p = 0.92$ V) in each organic molecule oxidation process over the bilayer compared to the same process on the Pt substrate. An important point can be highlighted: as discussed above, the hypothesis that these increases are related to a change in the surface area of the bilayer compared to Pt, or to a significant difference among the surfaces morphology, or even to the presence of ruthenium in the bilayer surface, is discarded. A difference was observed for the ethanol oxidation: there is a displacement of 110 mV (of 0.41 for 0.30 V) on the initial oxidation potential towards more negative values when the Ru/Pt bilayer was used compared to Pt (Fig. 6). Thus, the bilayer presents a different catalytic behavior from Pt.

Also, it is important to point out that the increases in the current densities observed for the bilayer continue during polarization experiments at constant potential for all oxidations of the small organic molecules studied. Fig. 7 shows the profiles obtained for ethanol oxidation over Pt (solid line) and over Ru/Pt bilayer (dashed line) in perchloric and in sulphuric media. As it can be observed, even for polarization times of 1200 s, the

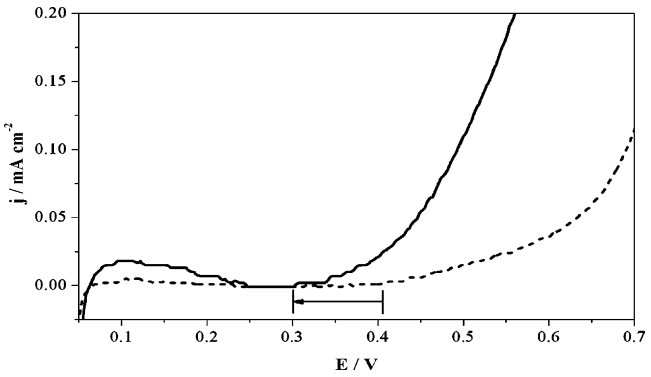

Fig. 6. Cyclic voltammograms presenting the shifting of the initial potential during ethanol oxidation over Ru/Pt bilayer electrodeposited over Pt (solid line) related to Pt (dashed line) in 0.1 mol L^{-1} $HClO_4$. Sweep rate = 20 mV s^{-1}.

current density is almost eight times higher for the Ru/Pt bilayer compared to the Pt substrate. This fact indicates that the bilayer structure decreases the poisoning effect of strongly adsorbed species on the surface generated during the oxidation process.

All data presented in Table 2 are statistically independent observations, i.e., the whole process – electrode and solution preparations – was repeated from the beginning. The experimental error presented in Table 2 is related to the influence of random factors associated with the whole process, the great sensitivity of the oxidation reactions on modifications of the surface being the most important one, even though the same procedure of surface preparation has been used. This behavior can be associated with the different crystallographic phase distribution produced during the electrode preparation [65]. It can also be observed that the supporting electrolyte influences the bilayer efficiency to the organic molecules oxidation process, with larger values of current density observed in perchloric media. It is known that the oxidation of organic molecules over Pt electrodes is quite sensitive to the nature of the supporting electrolyte [63,66–68]. Smaller currents are observed in H_2SO_4 solutions than in $HClO_4$ solutions. In a general way, the currents at lower potentials are

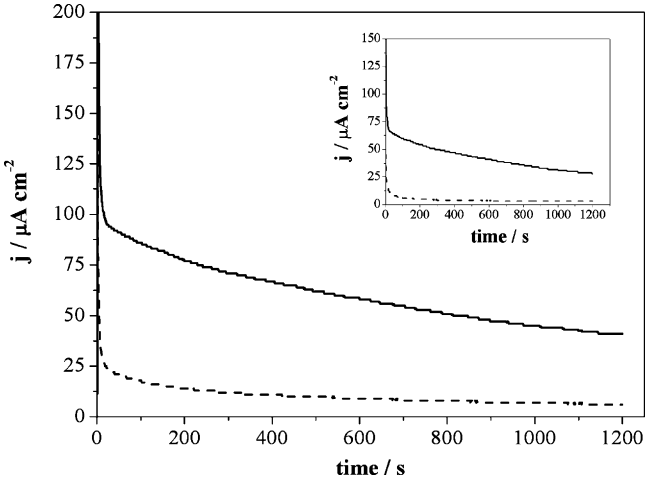

Fig. 7. Chronoamperometric measurements for ethanol oxidation on Pt (dashed line) and the bilayer Ru/Pt electrodeposited over Pt (solid line). E_{ox} = 0.5 V, time = 20 min, [CH_3COOH] = 0.5 mol L^{-1} in 0.1 mol L^{-1} $HClO_4$ and 0.1 mol L^{-1} H_2SO_4 (insert).

similar, or at least, of the same magnitude for both electrolytes, however a pronounced difference in the activity becomes evident at higher potentials. This effect has been attributed to an inhibition of the oxidation due to the specific adsorption of sulphate or bisulphate ions [69]. The anion effect on the organic molecules oxidation can also be observed in Fig. 5. The supporting electrolyte influences both the oxidation efficiency and the shape of the voltammetric profile (insert in Fig. 5). An exception is the formic acid oxidation, whose profile remains the same for both electrolytes and therefore is not influenced by anions adsorption [70].

The effect of the supporting electrolyte is also observed comparing the relative current density peak for the different processes observed. From a different point of view, the relationships between the current density peaks are different in the two electrolytes for ethanol oxidation, i.e., the ratio between current density peaks 1 and 2 in H_2SO_4 is 1.00 and the ratio between current density peaks 1 and 3 is 0.8. In $HClO_4$ media these ratios are 1.15 and 1.10, respectively. The same kind of behavior is observed for methanol but the ratios have different values. For formic acid, no electrolyte effect is observed. The bisulphate anions adsorption on polycrystalline Pt begins at the hydrogen region and extends to more positive potentials, reaching a maximum at 0.45 V [71]. The OH^- adsorption and formation of Pt oxides begins at lower potentials in perchloric that in sulphuric acid. The influence of bisulphate anions in the OH adsorption is generally attributed to the blockage of the Pt sites or OH_{ads} displacement by the bisulphate anions [72]. Perchlorate anions adsorption is weaker, since it appears adsorbed on polycrystalline Pt in the solvated form [73]. The chronoamperometric experiments also present that tendency of obtaining larger current density values for the oxidations when they are performed in an aqueous perchloric media (Fig. 7).

In summary, it is important to point out that the currents densities for the chronoamperometric experiments for ethanol oxidation using the bilayer system Ru/Pt are higher (43 μA cm^{-2}) than those ones obtained using the best electrocatalyst know PtRu alloys (32 μA cm^{-2}) [74], considering the applied potential (0.5 V), polarization time (20 min), ethanol concentration which is two times lower in this work (0.5 mol L^{-1}) and electrolyte solution (0.1 mol L^{-1} $HClO_4$). On the other hand, for methanol oxidation (0.5 mol L^{-1}) in 0.1 mol L^{-1} $HClO_4$ the Pt/Ru/Pt presents lower currents (26 μA cm^{-2}) than on PtRu alloys (180 μA cm^{-2}) [75]. Finally, for formic acid oxidation over the Pt/Ru/Pt the values of current densities during the chronoamperometric experiments are very high, 1.3 mA cm^{-2} (in perchloric acid) and 0.9 mA cm^{-2} (in sulphuric acid) approximately three times higher than on Pt.

4. Conclusions

In this work, a Ru/Pt bilayer was electrodeposited on a polycrystalline Pt substrate leading to the system Pt/Ru/Pt, which has different electrochemical properties compared to Pt. Both electrodes presented the same electroactive area. Although the Ru/Pt bilayer voltammetric profile was practically equal to the Pt in the blank solution, the response of the bilayer to organic

molecules oxidation was quite different. The oxidation current density was about three to four times higher for the bilayers. Other important effects are the displacements to more negative potentials on the CO peak potential and on the oxidation beginning in case of ethanol.

Acknowledgements

The authors wish to thank to FAPESP (05/0453-9, 04/04869-2 and 01/06029-3) CAPES and CNPq for the granted financial support.

References

[1] K. Kordesch, G. Simader, Fuel Cells and Their Applications, VCH, Weinheim, 1996.
[2] N. Giordano, E. Passalacqua, L. Pino, A.S. Aricó, V. Antonucci, M. Vivaldi, K. Kinoshita, Electrochim. Acta 36 (1991) 13.
[3] M.P. Hogarth, J. Munk, A.K. Shukla, A. Hamnett, J. Appl. Electrochem. 24 (1994) 85.
[4] T. Iwastita, J. Braz. Chem. Soc. 13 (4) (2002) 401.
[5] J.W. Long, R.M. Stroud, K.E. Swider-Lyons, D.R. Rolison, J. Phys. Chem. B 104 (2000) 9772.
[6] G.-Q. Lu, W. Chrzanowski, A. Wieckowski, J. Phys. Chem. B 104 (2000) 5566.
[7] T. Iwasita, Electrochim. Acta 47 (2002) 3663.
[8] F. Vigier, C. Coutanceau, F. Hahn, E.M. Belgsir, C. Lamy, J. Electroanal. Chem. 563 (2004) 81.
[9] P. Olivi, L.O.S. Bulhões, J.M. Leger, F. Hahn, B. Beden, C. Lamy, J. Electroanal. Chem. 370 (1994) 241.
[10] T. Iwasita, F.C. Nart, B. Lopez, W. Vielstich, Electrochim. Acta 37 (1992) 2361.
[11] S.L. Gojkovic, J. Electroanal. Chem. 573 (2004) 271.
[12] V.S. Bagotzki, Y.B. Vassileiv, Electrochim. Acta 12 (1967) 1323.
[13] V.S. Bagotzki, Y.B. Vassiliev, O.A. Kazova, J. Electroanal. Chem. 81 (1977) 229.
[14] R. Parsons, T. Van der Not, J. Electroanal. Chem. 257 (1988) 9.
[15] S. Wasmus, A. Küver, J. Electroanal. Chem. 461 (1999) 14.
[16] D. Kardash, C. Korzeniewski, N. Markovicǐ, J. Electroanal. Chem. 500 (2001) 518.
[17] J.-M. Léger, J. Appl. Chem. 31 (2001) 767.
[18] A.V. Tripković, K.Dj. Popović, J.D. Lović, V.M. Jovanović, A. Kowal, J. Electroanal. Chem. 572 (2004) 119.
[19] V.M. Schmidt, R. Ianniello, E. Pastor, S.R. González, J. Phys. Chem. 100 (1996) 17901.
[20] X.H. Xia, H.-D. Liess, T. Iwasita, J. Electroanal. Chem. 437 (1997) 233.
[21] T. Iwasita, E. Pastor, Electrochim. Acta 39 (1994) 531.
[22] M. Watanabe, S. Motoo, J. Electroanal. Chem. 444 (1998) 95.
[23] C. Panja, N. Saliba, B.E. Koel, Surf. Sci. 395 (1998) 248.
[24] J.P.I. De Souza, S.L. Queiroz, K. Bergamaski, E.R. Gonzalez, F.C. Nart, J. Phys. Chem. B 106 (2002) 9825.
[25] M. Watanabe, S. Motoo, J. Electroanal. Chem. 60 (1975) 267.
[26] R.T.S. Oliveira, M.C. Santos, B.G. Marcussi, P.A.P. Nascente, L.O.S. Bulhões, E.C. Pereira, J. Electroanal. Chem. 575 (2005) 177.
[27] R.T.S. Oliveira, M.C. Santos, B.G. Marcussi, S.T. Tanimoto, L.O.S. Bulhões, E.C. Pereira, J. Power Sources 157 (2006) 212.
[28] M.N. Baibich, J. Broto, A. Fert, F. Nguyen Van Dau, F. Petroff, P. Eitenne, G. Creuzet, A. Frederich, J. Chazelas, Phys. Rev. Lett. 61 (1988) 2472.
[29] B. Hammer, J.K. Norskov, Surf. Sci. 343 (1995) 211.
[30] K.W. Jacobsen, P. Stolze, J.K. Norskov, Surf. Sci. 366 (1996) 394.
[31] P.M.O. Edersen, S. Helveg, A. Ruban, I. Stensgaard, E. Laegsgaard, J.K. Norskov, F. Besenbacher, Surf. Sci. 426 (1999) 395.
[32] E. Christoffersen, P. Liu, A. Ruban, H.L. Skriver, J.K. Norskov, J. Catal. 199 (2001) 123.
[33] B. Hammer, Y. Morikawa, J.K. Norskov, Phys. Rev. Lett. 76 (1996) 2141.
[34] A. Ruban, B. Hammer, P. Stoltze, H.L. Skriver, J.K. Norskov, J. Mol. Catal. 115 (1997) 421.
[35] J. Zhang, M.B. Vukmirovic, Y. Xu, M. Mavrikakis, R.R. Adzic, Angew. Chem. Int. Ed. 44 (2005) 2132.
[36] J.F. Moulder, W.F. Stickle, P.E. Sobol, K.D. Bomben, Handbook of X-ray Photoelectron Spectroscopy, Physical Electronics, Inc., Eden Prairie, Minnesota, 1995.
[37] M. Krausa, W. Vielstich, J. Electroanal. Chem. 379 (1994) 307.
[38] T. Iwasita, H. Hoster, A. John-Anacker, W.F. Lin, W. Vielstich, Langmuir 16 (2000) 522.
[39] F.P. Gorstema, J.W. Cobble, J. Am. Chem. Soc. 83 (1961) 4317.
[40] W. Chrzanowski, A. Wieckowski, Langmuir 13 (1997) 5974.
[41] S.H. Bonilla, C.F. Zinola, J. Rodríguez, V. Díaz, M. Ohanian, S. Martínez, B.F. Giannetti, J. Colloid Interface Sci. 288 (2005) 377.
[42] J.C. Davies, B.E. Hayden, D.J. Pegg, M.E. Rendall, Surf. Sci. 496 (2002) 110.
[43] C. Bock, M.-A. Blakely, B. MacDougall, Electrochim. Acta 50 (2005) 2401.
[44] Z. Jusys, J. Kaiser, R.J. Behm, Electrochim. Acta 47 (2002) 3693.
[45] T.J. Schmidt, M. Noeske, H.A. Gasteiger, R.J. Behm, Langmuir 13 (1997) 2591.
[46] M.M. Hukovic, S. Omanovic, J. Mol. Catal. A Chem. 136 (1998) 75.
[47] S. Chen, M. Schell, J. Electroanal. Chem. 478 (1999) 108.
[48] J. Shin, W.J. Tornquist, C. Korzeniewski, C.S. Hoaglund, Surf. Sci. 364 (1996) 122.
[49] G.A. Camara, I. Iwasita, J. Electroanal. Chem. 578 (2005) 315.
[50] R. Ianniello, V.M. Schmidt, J.L. Rodriguez, E.P. Pastor, J. Electroanal. Chem. 471 (1999) 167.
[51] H.A. Gasteiger, N. Markovic, P.N. Ross, E.J. Cairns, J. Electrochem. Soc. 141 (1994) 1795.
[52] T. Zerihun, P. Grundler, J. Electroanal. Chem. 441 (1998) 57.
[53] L.-W.H. Leung, M.J. Weaver, J. Phys. Chem. 92 (1988) 4019.
[54] B. Ren, X.Q. Li, C.X. She, D.Y. Wu, Z.Q. Tian, Electrochim. Acta 46 (2000) 193.
[55] L.-W.H. Leung, M.J. Weaver, Langmuir 6 (1990) 323.
[56] Y. Xu, A. Armini, M. Schell, J. Electroanal. Chem. 398 (1995) 95.
[57] X.H. Xia, T. Iwasita, J. Electrochem. Soc. 140 (1993) 2559.
[58] S. Wasmus, W. Vielstich, Electrochim. Acta 38 (1993) 185.
[59] H. Kita, H.-W. Lei, J. Electroanal. Chem. 388 (1995) 167.
[60] B. Beden, J.M. Leger, C. Lamy, in: J.O. Bockris, B.E. Conway, R.E. White (Eds.), Modern Aspects of Electrochemistry, vol. 22, Plenum Press, New York, 1992, p. 97.
[61] S.G. Sun, J. Clavilier, A. Bewick, J. Electroanal. Chem. 240 (1988) 147.
[62] A. Capon, R. Parsons, J. Electroanal. Chem. 44 (1973) 239.
[63] G.-Q. Lu, A. Crown, A. Wieckowski, J. Phys. Chem. B 103 (1999) 9700.
[64] A. Wieckowski, J. Sobkowski, J. Electroanal. Chem. 63 (1975) 365.
[65] E.A. Batista, G.R.P. Malpass, A.J. Motheo, T. Iwasita, J. Electroanal. Chem. 571 (2004) 273.
[66] N. Markovic, P.N. Ross, J. Electroanal. Chem. 330 (1992) 499.
[67] H. Kita, Y. Gao, H. Hattori, J. Electroanal. Chem. 373 (1994) 177.
[68] E. Herrero, K. Franaszczuk, A. Wieckowski, J. Phys. Chem. 98 (1994) 5074.
[69] H. Kita, Y. Gao, H. Hattori, J. Electroanal. Chem. 373 (1994) 177.
[70] H. Okamoto, W. Kon, Y. Mukouyama, J. Phys. Chem. B 108 (2004) 4432.
[71] M.E. Gamboa-Aldeco, E. Herrero, P.S. Zelenay, A. Wieckowski, J. Electroanal. Chem. 348 (1993) 451.
[72] J.D. Lović, A.V. Tripković, S.Lj. Gojković, K.Dj. Popović, D.V. Tripković, P. Olszewski, A. Kowa, J. Electroanal. Chem. 581 (2005) 294.
[73] M.C. Santos, D.W. Miwa, S.A.S. Machado, Electrochem. Commun. 2 (2000) 692.
[74] G.A. Camara, R.B. Lima, T. Iwasita, Electrochem. Commun. 6 (2004) 812.
[75] E.A. Batista, H. Hoster, T. Iwasita, J. Electroanal. Chem. 554–555 (2003) 265.